JOURNAL OF PROPULSION AND POWER
Vol. 11, No. 2, March–April 1995

Effects of Applied Magnetic Fields on Performance of a Quasisteady Magnetoplasmadynamic Arcjet

Hirokazu Tahara,* Yoichi Kagaya,† and Takao Yoshikawa‡
Osaka University, Toyonaka, Osaka 560, Japan

A quasisteady magnetoplasmadynamic arcjet with applied magnetic fields was studied to clarify the influence of axial magnetic fields on the thruster performance and the discharge feature. Pulsed axial magnetic fields were applied by a few-turn coil, which was connected with a pulse-forming network independent of the main discharge circuit. An increase in axial-field intensity raised the discharge voltages at constant discharge currents below the limiting current with H_2, the mixture of $N_2 + 2H_2$ simulating fully decomposed hydrazine, and Ar. The thrust characteristics for H_2 and the mixture of $N_2 + 2H_2$ showed that there was the optimum axial-field intensity with which the maximum thrust was achieved for each gas, although at low discharge current levels for H_2 and Ar the thrusts increased with axial-field intensity. The discharges for all gases were inclined to occur more upstream with an increase in axial-field intensity. It was inferred that these effects of axial magnetic fields on the thruster performance and the arc feature were due to the rotating motion of $-J_r \times B_z$, i.e., swirl acceleration and enhanced thermalization.

Introduction

THE quasisteady magnetoplasmadynamic (MPD) arcjet is a promising propulsion device that utilizes principally electromagnetic acceleration of the interaction between the discharge current of kiloamperes and the self-induced azimuthal magnetic field. In this article the effect of axial magnetic fields on the thruster performance and the discharge feature is examined. The application of an axial magnetic field was expected to cause an azimuthal current and additional electromagnetic body forces in the discharge chamber.[1–5] In other words, the discharge feature and the acceleration mechanism are considered to change with an axial magnetic field.

When MPD arcjets were operated in a steady-state mode at low current levels below 3 kA in the 1960s, axial magnetic fields were applied in the discharge chamber with heavy solenoidal coils for the improvement of the thrust characteristics.[1–3] In previous papers[6–8] we proposed a practical application of axial magnetic fields in space to quasisteady self-field MPD arcjets in such a way that a few-turn coil, which was located outside the annular anode, was connected in series with a pulse-forming network (PFN) supplying main discharge powers, considering coil weight, extra power to the coil circuit, and thruster system integration. In this scheme, the applied-field intensity increased linearly with the discharge current. Then, we reported the effects of axial magnetic fields in series on the thruster performance, electrode erosion, and discharge stability. It was concluded that an axial-field application to self-field MPD arcjets caused the following merits: 1) an increase in thrust and thrust efficiency, 2) a decrease in electrode erosion, and 3) the achievement of stable operation at higher specific impulses.

In the present experiments, axial magnetic fields are applied in a self-field MPD arcjet chamber with a few-turn coil, which is connected with a PFN independent of the main discharge circuit; thus, the axial-field intensity can be varied in a constant discharge current operation. The discharge voltage and thrust characteristics are examined for variations of axial-field intensity at a same discharge current. In addition, current fractions on the anode are measured with a segmented anode to understand the influence of axial magnetic fields on the discharge feature; optical diagnostics in the discharge chamber are also conducted.

Experimental Apparatus

Figure 1a shows the configuration of the quasisteady MPD arcjet with applied magnetic fields used in the present study. The arcjet, which is called the MY-III arcjet, is provided with a straight-diverging anode made of copper. The anode nozzle is 58 mm in exit diameter and has a 20-deg half-angle. The anode is divided azimuthally into four parts; the slits between them are filled with ceramics as an electrically insulating and heat-resisting material. The azimuthal eddy current induced on the anode surface is cut by this method, and pulsed magnetic fields can penetrate quickly into the discharge chamber. The MY-III arcjet is equipped with ring coils outside the anode for the application of axial magnetic fields. A cylindrical cathode 17.5 mm in length and 9.5 mm in diam is made of thoriated tungsten.

The anode is also divided axially into six anode parts, which are electrically insulated to one another, to measure current distributions on the anode and to observe discharge features in the arcjet chamber. Thus, the current entering each anode segment is measured with a Rogowski coil. In inner discharge observation, an anode segment is removed, and a quartz glass tube is fitted to the position of the anode segment, as shown in Fig. 1b.

Propellants are injected with a cathode slit/anode slit ratio of 50/50 into the discharge chamber through a fast-acting valve (FAV) fed from a high-pressure reservoir. The rise time and width of the gas pulse, measured with a fast ionization gauge, are 0.5–1.0 and 6 ms, respectively. The mass flow rates are controlled by adjustment of the reservoir pressure and the orifice diameter of the FAV.

The main power-supplying PFN, which is capable of storing 62 kJ at 8 kV, delivers a single nonreversing quasisteady current of a maximum of 27 kA, with a pulse width of 0.6 ms. A vacuum tank 5.75 m in length and 0.6 m in diameter, where

Presented as Paper 91-073 at the AIDAA/AIAA/DGLR/JSASS 22nd International Electric Propulsion Conference, Viareggio, Italy, October 14–17, 1991; received June 19, 1992; accepted for publication July 20, 1994.

*Associate Professor, Faculty of Engineering Science, Department of Mechanical Engineering. Member AIAA.

†Assistant Engineer, Faculty of Engineering Science, Department of Mechanical Engineering.

‡Professor, Faculty of Engineering Science, Department of Mechanical Engineering. Member AIAA.

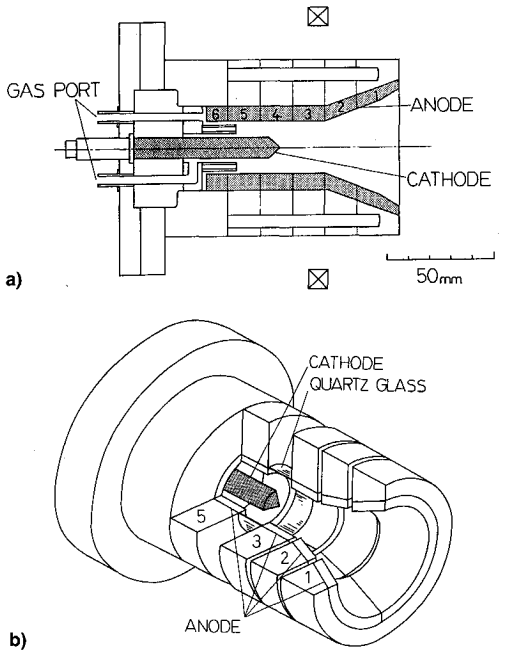

Fig. 1 Configuration of the MY-III MPD arcjet with applied magnetic field: a) cross-sectional view and b) cut sketch.

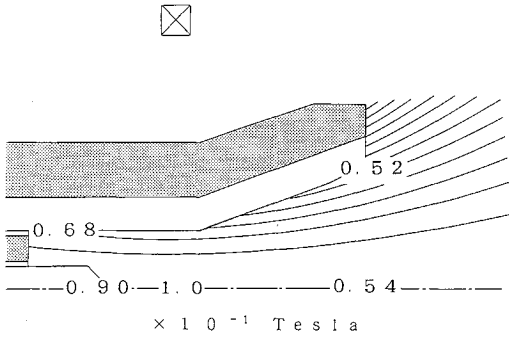

Fig. 2 Calculated intensities and the profile of applied magnetic field CL-type with 0.1 T at the center of the coil. The field intensity is variable.

the arcjet is fired, is evacuated to some 10^{-3} Pa prior to each discharge.

Discharge currents are measured by a Rogowski coil calibrated with a known shunt resistance. Voltage measurement is performed with a current probe (Iwatsu CP-502), which detects the small current bled through a known resistor (10 kΩ) between the electrodes.

Pulsed axial magnetic fields are applied with a few-turn coil, which is connected with a PFN independent of the main discharge circuit. The PFN is capable of delivering a quasisteady current of 8.5 kA with a pulse width of 1 ms at a charging voltage of 300 V. The applied-field intensity is proportional to the coil current, in other words the charging voltage. Hence, the axial-field intensity can be varied in a constant discharge current operation. The applied-field circuit is triggered before 0.35 ms of discharge start. The rise time of the applied magnetic fields in the discharge chamber was confirmed to be the same as that of the coil current with a $\dot{B}_z$ probe. Calculated magnetic field lines and field intensities, and the location of the coil are drawn in Fig. 2, where the field shape is called the CL-type. The CL type consists of a three-turn coil at a radius of 57 mm and an axial position of 14 mm downstream of the cathode tip. The axial-field intensity is varied up to 0.5 T at the axial position of the coil on the arcjet axis, and the field lines gradually expand downstream. It is noted for no axial magnetic field that the azimuthal self-field intensities, which are measured with a $\dot{B}\theta$ probe, at a discharge current of 10 kA for a mixture of N_2 + $2H_2$ simulating fully decomposed hydrazine, are about 0.18 T near the cathode tip and about 0.03 T at the nozzle end. The self-field intensities are compared with the axial-field ones.

Thrusts are measured by a pendulum method. The MPD arcjet and FAV are mounted on a thrust stand suspended with a brass bar, and the position of the thrust stand is detected by a linear differential transformer. The thrusts are calibrated before and after a series of experiments by applying impulses of known magnitude using small steel balls in an atmospheric-pressure environment. Apparent thrusts, i.e., errors due to the pulsed application of axial magnetic fields are omitted in such a way that the oscillations under axial-field application are evaluated both without main discharges and in electrically short conditions of the main discharge circuit. The thrust due to arc discharge alone is discussed, i.e., it is yielded by subtracting the thrust due to cold gas flow from the thrust measured in the arc operation.

Emission spectroscopy is conducted as reliable plasma diagnostics in the arcjet chamber.[9] Light comes from the plasma in the discharge chamber through a quartz glass slit 0.5 mm in width between anode segments, as shown in Fig. 1. The emission is collected by a lens of 300 mm in focal length and is introduced into a monochrometer of diffraction grating type (Simadzu GE-100: 1.66 nm/mm; 600 grooves/mm). The spectral intensities measured in this experiment are line-of-sight values, measured by looking through the arc from the side perpendicular to the centerline of the arcjet. For line-of-sight measurements, the intensity values correspond to integrated values of intensity as a function of position. We determine the radial-dependent emission coefficient from the measured spectral intensities using widely known inverse Abel transformations under the assumption of axisymmetric and optically thin plasmas in the arcjet chamber.

Experimental Results and Discussion

The present experiments are carried out using H_2, the mixture of N_2 + $2H_2$, and Ar gases. The mass flow rates are determined from the theories of Alfvén's critical velocity and self-field electromagnetic acceleration, in which the corresponding critical current is about 10 kA.[7,9,10]

Influences of Axial Magnetic Fields on Operational Characteristics

Figure 3a shows the discharge voltage vs current characteristics for H_2 under the application of the axial magnetic field CL-type, in which the axial-field intensities at the center of the coil are represented. Figures 3b, 4a, and 4b show the relations between the rate of increase in the voltage with the axial magnetic field on the voltage only with the self-field and the axial-field intensity for H_2, the mixture of N_2 + $2H_2$, and Ar, respectively. In general, when an axial magnetic field is applied, the discharge voltage is expected to increase because of an additional back voltage.[1-5] Correspondingly, these figures show that an increase in axial-field intensity raises the discharge voltages for all propellants at low discharge current levels. However, the voltage characteristics have poor dependences on axial-field intensity at high discharge currents. The voltages near the limiting operations are considered to be dominated by other effects on the so-called onset phenomena, such as anode spot generation and plasma instabilities.[9,10]

Figure 5a shows the thrust vs discharge current characteristics for H_2 under the application of the axial magnetic field CL-type. Figures 5b, 6a, and 6b show the relations between the rate of increase in the thrust with the axial magnetic field on the thrust only with the self-field and the axial-field intensity for H_2, the mixture of N_2 + $2H_2$, and Ar, respectively. The thrust characteristics for H_2 and the mixture of N_2 + $2H_2$ show that there is the optimum axial-field intensity, with which the maximum thrust is achieved, for each gas in the same

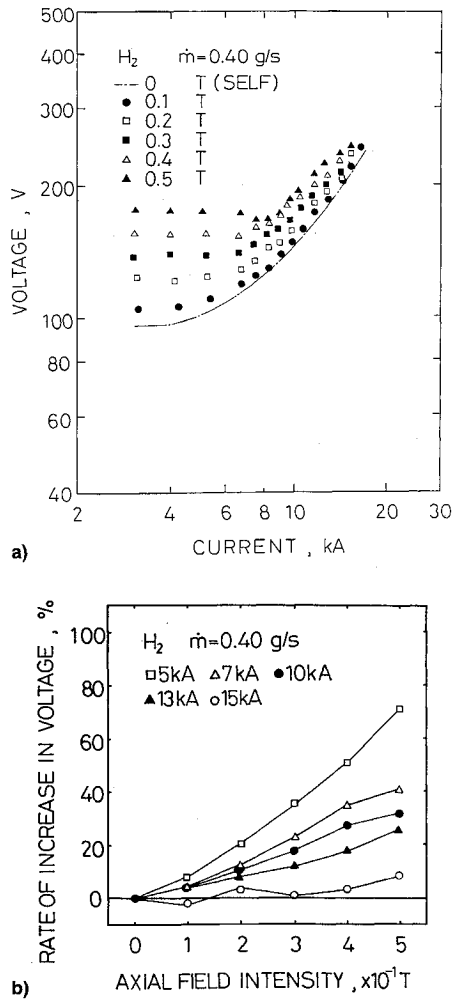

Fig. 3 Discharge voltage vs current characteristics under the application of axial magnetic field CL-type, and the relation between the rate of increase in voltage with axial-field on voltage only with self-field and axial-field intensity for H_2 with 0.40 g/s. The axial-field intensities at the center of the coil are represented: a) V vs J and b) rate of V increase vs B_z characteristics for H_2 with 0.40 g/s.

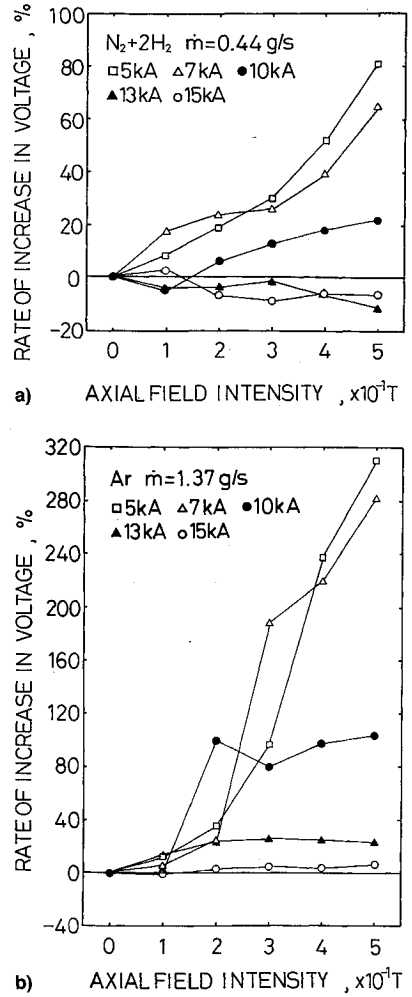

Fig. 4 Relations between the rate of increase in voltage with axial-field on voltage only with self-field and axial-field intensity for the mixture of N_2 + $2H_2$ with 0.44 g/s and Ar with 1.37 g/s. The axial-field intensities at the center of the coil are represented. The discharge voltages for the mixture of N_2 + $2H_2$ only with the self-field at 5, 7, 10, 13, and 15 kA are 68.4, 82.2, 135.2, 208.4 and 230.0 V, respectively, and the voltages for Ar are 30.6, 36.2, 77.2, 130.8 and 167.2 V, respectively. Rate of V increase vs B_z characteristics for a) the mixture of N_2 + $2H_2$ with 0.44 g/s and b) for Ar with 1.37 g/s.

current operations, except at 5 kA for H_2 and at 13 and 15 kA for the mixture of N_2 + $2H_2$. They are 0.3 T for H_2 and 0.1 T for the mixture of N_2 + $2H_2$. Strong axial magnetic fields do not contribute to the improvement of the thrust characteristics. Particularly, at axial-field intensities above 0.3 T, the thrusts for the mixture of N_2 + $2H_2$ are much smaller than those only with the self-field. Axial-field application is found to be effective in low current operations for all propellants. An increase in axial-field intensity enlarges the thrusts for H_2 at 5 kA, and for Ar at 5 and 7 kA, and the thrusts at 0.5 T for H_2 and Ar increase up to about 35 and 30%, respectively.

The thrust efficiencies for the mixture of N_2 + $2H_2$ reach the maximum values with an axial-field intensity of 0.1 T at constant specific impulses or discharge currents below about 10 kA. However, the axial-field application for H_2 and Ar hardly contributes to the enhancement of thrust efficiency at constant specific impulses because of increases in the discharge voltages, although the thrusts increase with the axial magnetic field at constant discharge currents.

Discharge Feature and Acceleration Mechanism Under Axial-Field Application

The discharge voltage and thrust characteristics under the application of the axial magnetic field are expected to depend strongly on current distributions in the discharge chamber. We infer the current conduction patterns from the current entering each anode segment as shown in Fig. 1. The current fraction characteristics on the anode are shown in Figs. 7–9. For all gases an increase in axial-field intensity increases the current fractions on the more upstream segments; i.e., the discharges are expected to occur more upstream, although for H_2 at 5 kA with an increase from 0.2 to 0.3 T and at 10 kA with 0.3–0.4 T, the discharges are inclined to occur more downstream as shown on the anode segments 2 and 3.

The inferred current distributions are in agreement with discharge observations in the arcjet chamber.[9] Also, it is noted at segment 3 of the same axial position of the coil, where the maximum field intensity is given in the discharge chamber, that the current fractions at 10 kA are largest with 0.3 T for H_2 and with 0.1 T for the mixture of N_2 + $2H_2$, with which the thrusts are maxima as shown in Figs. 3b and 4a. It will be explained later that thrust generation under axial-field application is related closely with the current pattern in the discharge chamber.

The upstream movement of the current conduction zone with the axial magnetic field is considered to exist because of enhanced Joule heating, as described in Refs. 1, 6, and 7. As for H_2 at 5 kA with 0.2–0.3 T, and at 10 kA with 0.3–0.4 T, the downstream transitions were reported in steady-state arcjet operations with strong axial magnetic fields[2–5]; i.e., the cur-

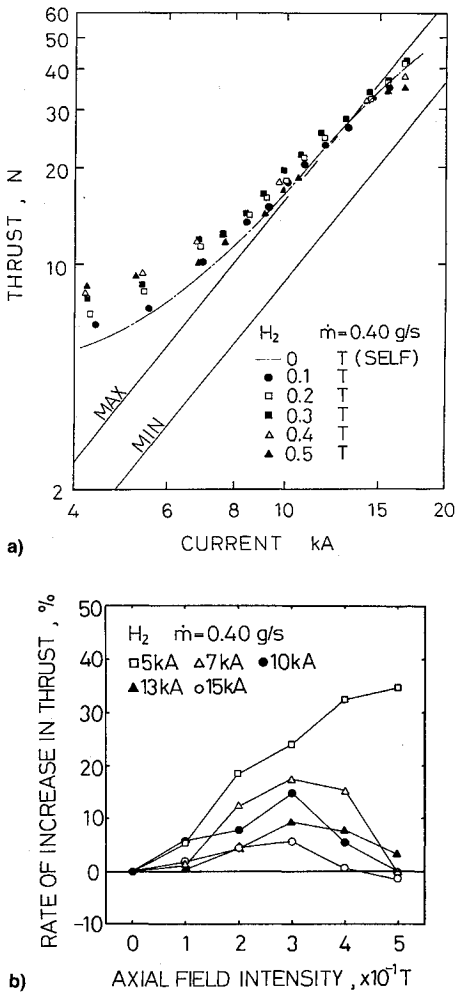

Fig. 5 Thrust vs discharge current characteristics under the application of axial magnetic field CL-type, and the relation between the rate of increase in thrust with axial-field on thrust only with self-field and axial-field intensity for H_2 with 0.40 g/s. The axial-field intensities at the center of the coil are represented: a) T vs J characteristics for H_2 with 0.40 g/s. The solid lines represent theoretical predictions of self-field electromagnetic acceleration. MAX: $T_m = 10^{-7}[\ell_n(r_a/r_c) + 3/4]J^2$ with $r_a/r_c = 12.5/4.75$; MIN: $T_m = 10^{-7}[\ell_n(r_a/r_c)]J^2$; and the b) rate of T increase vs B_z characteristics for H_2 with 0.40 g/s.

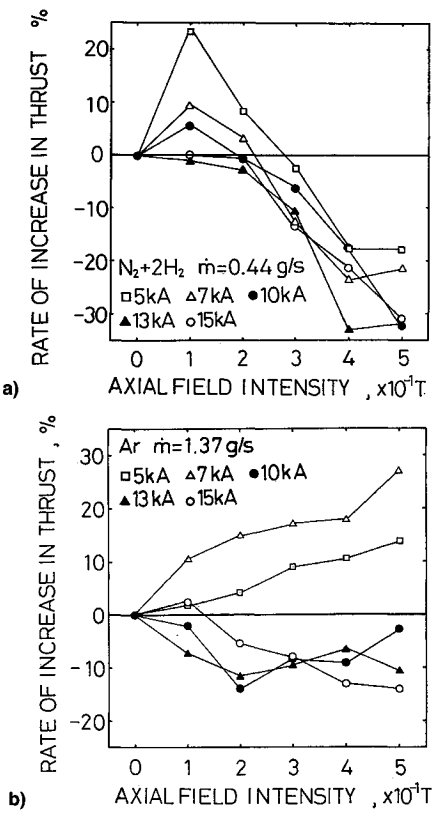

Fig. 6 Relations between the rate of increase in thrust with axial-field on the thrust only with self-field and axial-field intensity for the mixture of N_2 + $2H_2$ with 0.44 g/s and Ar with 1.37 g/s. The axial-field intensities at the center of the coil are represented. The thrusts for the mixture of N_2 + $2H_2$ only with the self-field at 5, 7, 10, 13, and 15 kA are 3.94, 6.18, 9.46, 17.15, and 25.11 N, respectively, and the thrusts for Ar are 3.31, 4.36, 9.35, 15.40, and 21.80 N, respectively. Rate of T increase vs B_z characteristics for a) the mixture of N_2 + $2H_2$ with 0.44 g/s and b) for Ar with 1.37 g/s.

rent path under axial-field application is inclined to be extended downstream outside the discharge chamber because of smooth motions of charged particles along the axial-field lines when the azimuthal self-field intensity is neglected compared with the axial-field intensity. Hence, axial-field application is expected to drastically change the arc feature in the discharge chamber.

The current fractions on anode segment 1 for most of field-applied operations decrease compared with those only with the self-field. As a result, the current concentration at the anode exit is relaxed under the application of the axial magnetic field, and anode erosion is expected to be reduced. Furthermore, it is noticed that for every gas there exists the current entering anode segment 6, which covers the space upstream outside the main discharge chamber as shown in Fig. 1a. This feature makes us expect the existence of the current along the insulator and floating electrodes at the upstream end of the discharge chamber, which may bring about severe erosion at the edge of the cathode.

Figures 10–12 show the radial profiles of the electron temperature in a slit between segments 3–4 at 10 kA for H_2, the mixture of N_2 + $2H_2$, and Ar. The electron temperature is estimated from measured radial-dependent spectral intensities under the assumption of a Boltzmann equilibrium distri-

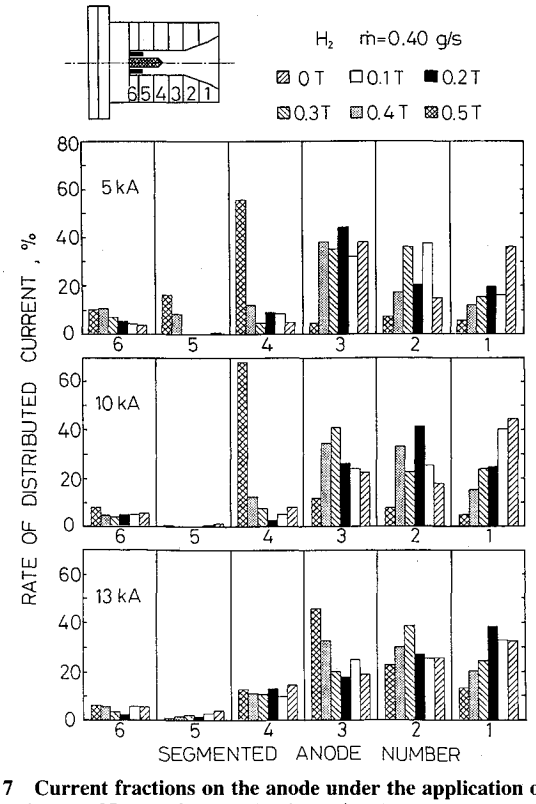

Fig. 7 Current fractions on the anode under the application of axial magnetic field CL-type for H_2 with 0.40 g/s. The axial-field intensities at the center of the coil are represented.

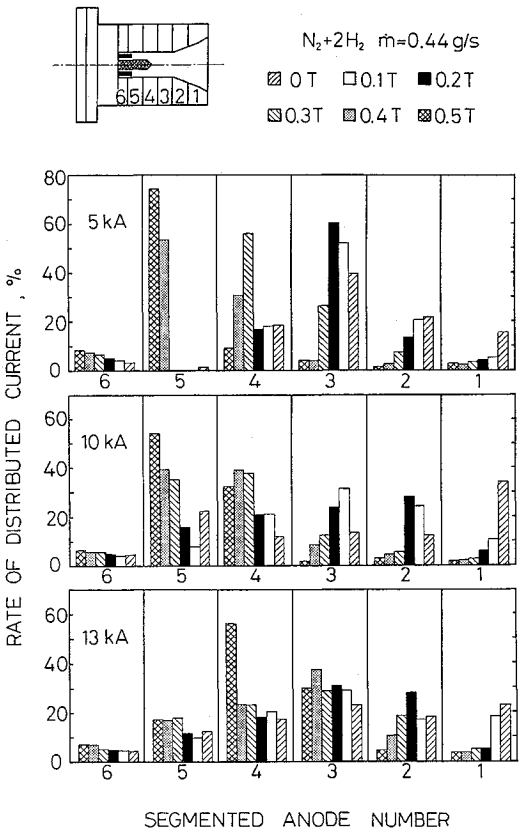

Fig. 8 Current fractions on the anode under the application of axial magnetic field CL-type for the mixture of N_2 + $2H_2$ with 0.44 g/s. The axial-field intensities at the center of the coil are represented.

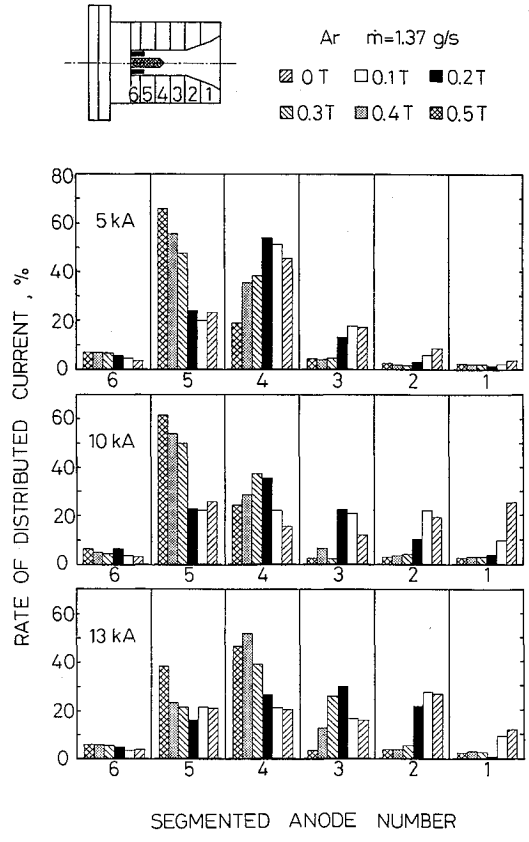

Fig. 9 Current fractions on the anode under the application of axial magnetic field CL-type for Ar with 1.37 g/s. The axial-field intensities at the center of the coil are represented.

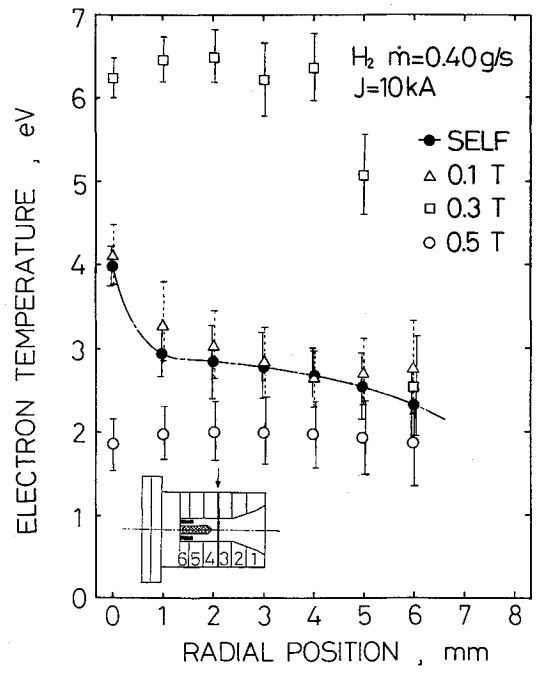

Fig. 10 Radial profiles of electron temperature in the arcjet chamber under the application of axial magnetic field CL-type for H_2 with 0.40 g/s at a discharge current of 10 kA. The axial-field intensities at the center of the coil are represented.

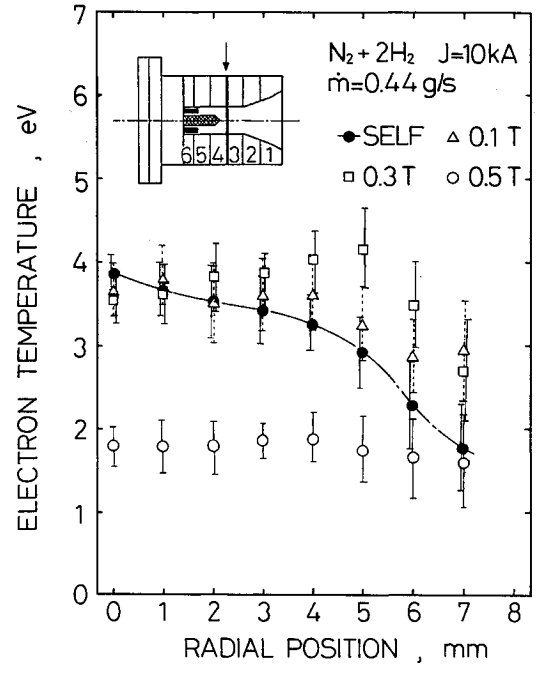

Fig. 11 Radial profiles of electron temperature in the arcjet chamber under the application of axial-magnetic field CL-type for the mixture of N_2 + $2H_2$ with 0.44 g/s at a discharge current of 10 kA. The axial-field intensities at the center of the coil are represented.

bution between electronically excited states.[9] The spectra used for the mixture of N_2 + $2H_2$ are nitrogen atom-ion ones, and for Ar, ArII lines are used. The profiles are almost flat for H_2 with 0.3 T and for the mixture of N_2 + $2H_2$ with 0.1 and 0.3 T, with high-temperature levels from the center to about 4 mm, although only with the self-field the electron temperatures gradually decrease in the positive radial direction. Thus, there exist the radially broad, high-temperature regions with the axial magnetic fields, particularly for H_2 with 0.3-T high-electron temperatures over 6 eV being achieved. This is expected to be mainly because of Joule heating enhanced by

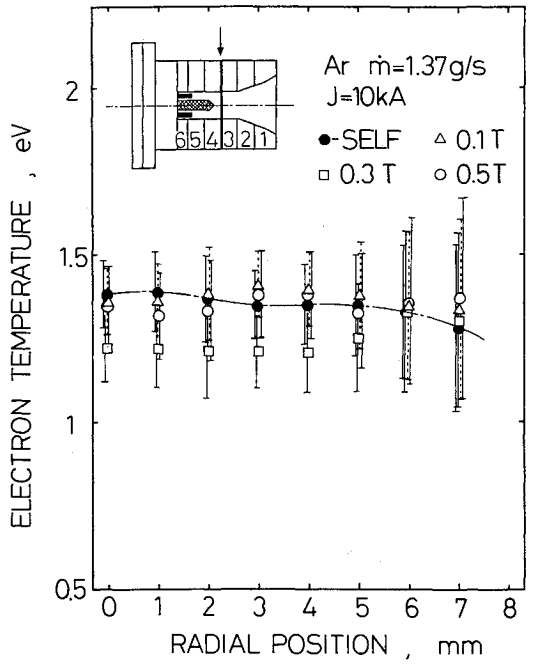

Fig. 12 Radial profiles of electron temperature in the arcjet chamber under the application of axial-magnetic field CL-type for Ar with 1.37 g/s at a discharge current of 10 kA. The axial-field intensities at the center of the coil are represented.

the application of the axial magnetic fields. On the other hand, the temperatures for H_2 and the mixture of $N_2 + 2H_2$ with 0.5 T, and for Ar with every axial-field intensity, are smaller than those only with the self-field since most of the discharge current with the axial field is distributed in the upstream region of measurement position.

We roughly estimate thrust components due to self-field acceleration, swirl one, and Hall one using the measured current fractions on the anode and previous diagnostic data.[1-3,6,7,9] The thrusts of pumping and blowing by the self-field decrease with axial-field intensity at a same discharge current because the discharge current distribution moves more upstream. On the other hand, an increase in axial-field intensity enlarges the thrust component of swirl acceleration, and the thrust of Hall one is very small compared with other thrust components. Hence, the estimated total thrusts for H_2 and the mixture of $N_2 + 2H_2$ indicate peak characteristics on axial-field intensity, which agrees with the measured thrust characteristics as shown in Figs. 5b and 6a.

Conclusions

From the present experiments with the applied-field MPD arcjet, the following results were obtained:

1) The discharge voltage increased with axial-field intensity at low discharge current levels.

2) The thrust characteristics for H_2 and the mixture of $N_2 + 2H_2$ showed that there was the optimum axial-field intensity with which the maximum thrust was achieved for each gas, although for H_2 and Ar at low discharge current levels the thrusts increased with axial-field intensity.

3) The discharges for most of the operational conditions occurred more upstream with an increase in axial-field intensity, resulting in broad high-temperature distributions in the discharge chamber for H_2 and the mixture of $N_2 + 2H_2$.

4) It was inferred that the changes of the thruster performance and the arc feature by axial-field application were due to the rotating motion of $-J_r \times B_z$, i.e., swirl acceleration and enhanced thermalization.

References

[1]Patrick, R. M., and Schneiderman, A. M., "Performance Characteristics of a Magnetic Annular Arc," *AIAA Journal*, Vol. 4, No. 2, 1966, pp. 283–290.

[2]Nerheim, N. M., and Kelly, A. J., "A Critical Review of the Magnetoplasmadynamic (MPD) Thruster for Space Application," Jet Propulsion Lab., TR 32-1196, Feb. 1968.

[3]Fradkin, D. B., Blackstock, A. W., Roehling, D. J., Stratton, T. F., Williams, M., and Liewer, K. W., "Experiments Using a 25-kW Hollow Cathode Lithium Vapor MPD Arcjet," *AIAA Journal*, Vol. 8, No. 5, 1970, pp. 886–894.

[4]Myers, R. M., Mantenieks, M., and Sovey, J., "Geometric Effects in Applied-Field MPD Thrusters," AIAA Paper 90-2669, July 1990.

[5]Sasoh, A., and Arakawa, Y., "Electromagnetic Effects in an Applied-Field Magnetoplasmadynamic Thruster," *Journal of Propulsion and Power*, Vol. 8, No. 1, 1992, pp. 98–102.

[6]Tahara, H., Kagaya, Y., and Yoshikawa, T., "Quasisteady Magnetoplasmadynamic Thruster with Applied Magnetic Fields for Near-Earth Missions," *Journal of Propulsion and Power*, Vol. 5, No. 6, 1989, pp. 713–717.

[7]Tahara, H., Sasaki, M., Kagaya, Y., and Yoshikawa, T., "Thruster Performance and Acceleration Mechanisms of a Quasi-Steady Applied-Field MPD Arcjet," AIAA Paper 90-2554, July 1990.

[8]Yoshikawa, T., Kagaya, Y., and Tahara, H., "Continuous Operational Tests of a Quasi-Steady MPD Arcjet System," Paper 91-075, Oct. 1991.

[9]Tahara, H., Yasui, H., Kagaya, Y., and Yoshikawa, T., "Experimental and Theoretical Researches on Arc Structure in a Self-Field Thruster," AIAA Paper 87-1093, May 1987.

[10]Yoshikawa, T., Kagaya, Y., and Kuriki, K., "Thrust and Efficiency of the K-III MPD Thruster," *Journal of Spacecraft and Rockets*, Vol. 21, No. 5, 1984, pp. 481–487.